Montogue

Quiz EG1
Wind Energy and Wind Turbines

Lucas Monteiro Nogueira

Problems

Problem 1

Regarding the theory of wind energy, are the following statements true or false?

1.( ) A wind turbine operates year-round at a rated power of 2 MW. If, over the course of one year, the turbine produced 3600 MWh, its capacity factor is greater than 24%.

2.( ) The following figure is a generic power curve for a typical HAWT. The horizontal and vertical axes measure wind speed and power converted, respectively. With reference to this graph, the power converted when the turbine is subjected to a wind speed of 10 m/s can be gleaned to be greater than 700 kW.

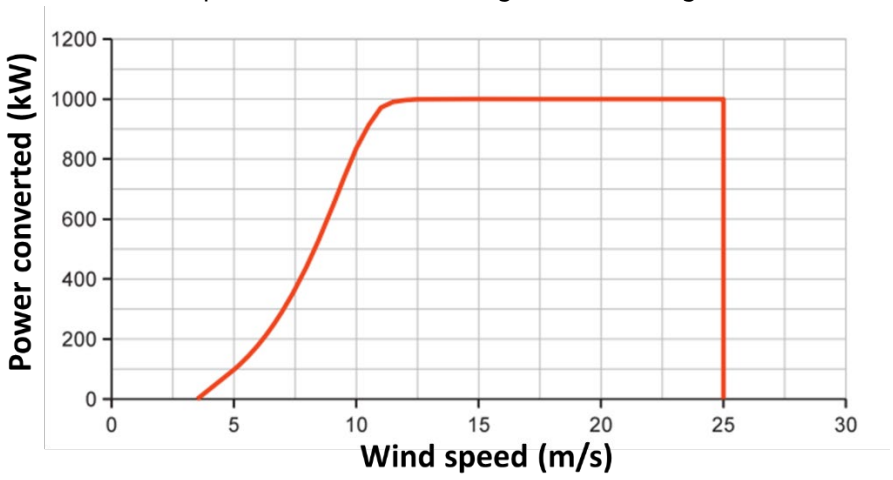

3.( ) Air flows across the rotor plane of a HAWT at a mean streamwise velocity of 10 m/s. The standard deviation of velocity measurements is 2 m/s. It follows that the turbulence intensity for this flow field is greater than 30%.

4.( ) Most modern wind turbine blades are made from glass fiber- and carbon fiber-reinforced composites. One important reason why these materials are preferred over other alternatives is their excellent fatigue resistance, which is superior to those of, say, mild steel or wood-epoxy laminate.

Recommended book: Anderson (2020).

Although early wind energy research was based on airfoil series originally designed for aviation purposes, several workers have since proposed airfoil families specifically tailored for the wind community. One example is the DU series of airfoils, developed at Delft University of Technology and summarized in Timmer and van Rooij (2003).

5.( ) One of the airfoils in the DU family is DU 93-W-210; the first two digits indicate 10 times the maximum airfoil thickness in percent of the chord, therefore the airfoil in question has a maximum thickness of 9.3%. ■ **(A black square indicates the end of a multi-paragraph statement.)**

Recommended research: Timmer and van Rooij (2003).

Although it appears that minimizing the number of blades in a HAWT may lead to the best turbine design, it has been shown that aerodynamic performance does increase with blade number albeit with diminishing returns. Increasing solidity should also increase torque for a given rotational speed, thereby increasing power output.

6.( ) Aiming to quantify the effects of solidity and blade number on the aerodynamic characteristics of HAWTs, Duquette and Visser (2003) conducted a numerical study using blade element momentum and lifting-line wake models. They found that power coefficients were optimum for designs with three blades and solidity ranging from 3 to 8%. ■

Recommended research: Duquette and Visser (2003).

7.( ) Traditionally, wind shear (i.e., variation of wind speed with atmospheric altitude) has been modeled with simple power laws or log laws. Ray *et al.* (2006) put these models to the test by assessing their performance when compared to wind velocity data for different types of terrain. Both models fared well in flat sites and especially in sites with hills, but in the latter case power-law models were found to be more accurate.

Recommended research: Ray *et al.* (2006).

8.( ) Dolan and Lehn (2006) developed a model that relates wind shear and tower shadow effects to dynamic torque oscillation in a three-bladed wind turbine. Those authors found that total 3*p* torque pulsation is more prominently affected by tower shadow phenomena than by wind shear.

Recommended research: Dolan and Lehn (2006).

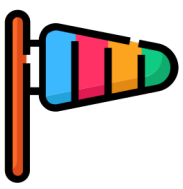

9.( ) Meteorological tower measurements are the industry standard for wind resource assessment in siting of turbine farms. Usually, anemometers are placed on horizontal booms that are attached to the wind turbine tower at several elevations. Due to the directional variability of the wind, anemometers are subjected to winds from all directions. In many cases, the anemometers are placed in the wake of the tower and hence may yield measurements which are under-representations of true wind speed. In view of these potential problems, Orlando *et al.* (2011) performed full-scale tests to study the effect of tower shadowing on cup anemometer wind speed readings in the wake of common tower geometries. Orlando's group found a significant wind speed deficit when anemometers are placed in the wake of the tower; crucially, measured velocity deficits were greatest when the centerline of the cup anemometer was directly inline with the centerline of the tower.

Recommended research: Orlando *et al.* (2011).

Instead of limiting the power output using pitch or stall regulation, engineers could resort to dynamic control of blade yaw. In normal pitch- or stall-regulated facilities, it is common to have a yaw drive which is constantly trying to rotate the nacelle to minimize the yaw misalignment in order to have the air flow adequately across the rotor disc. In a yaw-controlled machine, the rotor is turned out of the wind in high winds to limit the airflow through the rotor and thus the power extraction.

To date, very few prototypes of yaw-controllable turbines have been deployed. Gebraad *et al.* (2014) developed a high-fidelity CFD wind plant model to show that total electrical energy production can be optimized by changing the yaw in each turbine. In Gebraad's model yaw control was used to change the direction and velocity of the wake forming behind each turbine in the wind plant.

10.( ) Not only does the Gebraad *et al.* (2014) yaw-control model increase the energy production of the CFD-simulated wind plant, it also reduces mechanical loads on the turbines as an additional effect. ■

Recommended research: Gebraad *et al.* (2014).

11.( ) Yang *et al.* (2019) tackled the problem of wind farm layout optimization, a topic that has drawn the interest of several research groups in recent years. Yang's team introduced a novel objective function that, when optimized, yielded uniform wake effects within individual turbines. Importantly, Yang's objective function was implemented with a particle swarm optimization (PSO) algorithm.

Recommended research: Yang *et al.* (2019).

Direct numerical modelling of turbine rotors constitutes the most accurate CFD approach to wind energy. However, the computational burden associated with these methods is often immense.

12.( ) Some of the first simulations with direct modelling for wind energy applications were reported by Sørensen and Hansen (1998), who adopted an incompressible RANS solver with a rotating frame of reference and boundary-layer turbulence represented by the *SST k-ω* eddy viscosity model. Sørensen's group went on to apply their numerics to simple wind turbine problems and compare their results to measurements of mechanical power in two rotors; agreement was generally excellent, especially for air speeds greater than 10 m/s, which corresponded to intensified flow separation and turbulence. ■

Recommended research: Sørensen and Hansen (1998).

In September 2008, typhoon Jangmi struck Taiwan with winds exceeding 190 km/h. Among the infrastructure affected by the typhoon were the wind turbines in Changhua Coast Industrial Park, located in the central part of the island. Chou *et al.* (2013) investigated the blades of turbines that failed during Jangmi and complemented their research with other turbine failure data available at the time.

13.( ) Interestingly, Chou's review and computational model suggested that blades can effectively resist winds much greater than those registered during Jangmi, hence the cause of failure in the Changhua Park turbines had to be something else than mere greater-than-expected wind loads. ■

Recommended research: Chou *et al.* (2013).

Li *et al.* (2014) assessed the problem of icing on wind turbine airfoils. Li's group performed wind tunnel tests with a NACA 7715 airfoil and went on to calculate icing accretion rate and icing area. Those authors showed that icing accretion is more intense at high wind speeds. Moreover, at the same wind speed, icing accretion is mainly dependent on angle of attack.

14.( ) One important drawback of the Li *et al.* (2014) study is that their wind tunnel experiments were conducted in the summer, hence the air fed to the tunnel apparatus was unusually warm and did not replicate the cold atmosphere at which turbine blade icing typically takes place. ■

Recommended research: Li *et al.* (2014).

Aerodynamic losses due to blade surface roughness have become an emerging research topic in arid regions such as Egypt, where storms carrying large amounts of sand and dust are common meteorological events.

15.( ) Mendez *et al.* (2015) used a CFD code to study the performance of S809 and NACA 0012 airfoils in both clean and rough conditions. Mendez's group simulated flow across these foils at a range of Reynolds numbers and found that as *Re* increased, the maximum lift coefficient observed in the blade decreased and the minimum drag coefficient increased due to growing surface roughness. This response was monotonic, i.e., maximum C_L always decreased and minimum C_D always increased in response to rising Reynolds number, be it for clean or rough airfoil surfaces. ■

Recommended research: Mendez *et al.* (2015); see also the review by Zidane *et al.* (2016).

Raindrop impact is another important source of wind turbine damage. During rainfall, raindrops are carried by the wind and may collide with turbine blades at extremely high speeds. In the long run, raindrop wear translates into increased surface roughness and loss of aerodynamic performance.

Eisenberg *et al.* (2018) conducted a model-driven study of raindrop erosion on HAWT blade surfaces. Eisenberg's group combined a leading-edge erosion forecast model and an efficiency reduction model to assess annual energy production loss over time.

16.( ) One important feature of Eisenberg's model is that it does not account for very small drop diameters. ■

Recommended research: Eisenberg *et al.* (2018).

The impact of HAWTs on flying wildlife remains an active research topic. For instance, while loss of bat populations has been observed in wind energy installations, there is no consensus on how bats are struck down by turbines, with some arguing for simple mechanical impact and others suggesting that death could be ascribed to barotrauma – i.e., hemorrhaging as a result of sudden drop in air pressure.

17.( ) At any rate, it is certain that most instances of collisions between bats and turbine blades have been registered when the turbines are operational rather than standing at rest. ■

Recommended research: Schuster *et al.* (2015).

Problem 2

The wind velocity at 10 m height in a meteorological observatory is 8 m/s. What is the velocity at 35 m height at a wind turbine site having similar wind profile if the log-law is valid? The roughness heights at the observatory and wind turbine site are 0.05 m and 0.12 m, respectively. Assume that the wind velocity is not affected by surface conditions beyond a height of 60 m above ground level.

(A) 8.65 m/s
(B) 9.78 m/s
(C) 10.9 m/s
(D) 12.1 m/s

Problem 3

A wind turbine of the two-blade propeller type is designed to have its maximum power coefficient value at a tip-speed ratio, *TSR*, equal to 5 when the wind velocity is 8 m/s. If the blade diameter is 30 m, what is the rotational speed?

(A) 10.5 rpm
(B) 15.5 rpm
(C) 20.5 rpm
(D) 25.5 rpm

Problem 4

A wind turbine unit is rated at 2 MW when operating at a wind speed of 12 m/s. The stage efficiencies are gearbox efficiency η_{gb} = 0.95, generator efficiency η_g = 0.90, and turbine efficiency C_p = 0.28; all other efficiency metrics are equal to one. What is the necessary swept area? Use 1.225 kg/m^3 as the air density.

(A) 6900 m^2
(B) 7910 m^2
(C) 9000 m^2
(D) 9610 m^2

Problem 5

A certain wind turbine is rated at 1.8 MW. The blade diameter is 50 m and the rated wind speed is 14 m/s. The gearbox and generator efficiencies are both equal to 0.98; all other efficiency metrics are equal to unity. What is the power coefficient of the turbine? Take ρ = 1.225 kg/m^3 as the density of air.

(A) 0.358
(B) 0.433
(C) 0.501
(D) 0.567

Problem 6

A wind turbine rated at 1 MW and power coefficient $C_{p,\text{rated}}$ = 0.2 operates in a constant freestream airspeed of 15 m/s. Taking ρ = 1.225 kg/m^3 as the air density, The radius of the rotor recommended for this turbine is:

(A) 18.4 m
(B) 22.1 m
(C) 27.7 m
(D) 31.0 m

Problem 7

The following figure shows a stream-tube/actuator disc model of a wind turbine. Assume that the actuator disc has a radius of 5 m; the freestream wind speed is V_∞ = 8 m/s. Use ρ_∞ = 1.225 kg/m^3 as the air density.

Part 1: Estimate the maximum power that can be extracted by the idealized wind turbine.

Part 2: Determine the velocity at the actuator disc and in the wake.

Part 3: Determine the areas A_∞ and A_w.

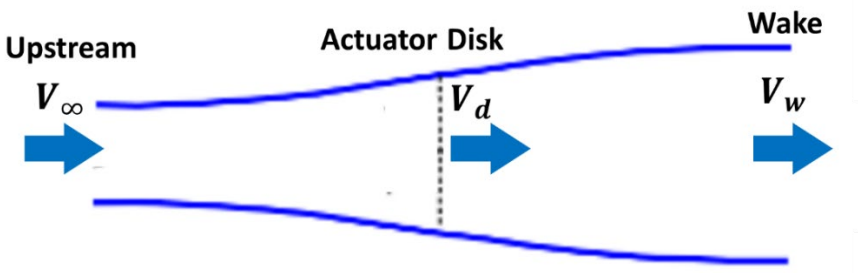

Problem 8

A generator driven by a HAWT is required to deliver 1.2 MW of power at the generator terminals. The turbine is a two-blade propeller rotating about a horizontal axis and the maximum permitted shear stress of the turbine shaft is 60 MPa. The rotor is designed to operate at a rotational speed of 20 rpm. The overall efficiency of the turbine is 0.40, and the air density may be taken as 1.225 kg/m^3.

Part 1: Assuming the turbine delivers its rated power at a wind average speed of 32 km/h, determine the corresponding diameter of the propeller and its tip speed ratio.

Part 2: Calculate the torque on the turbine shaft and the necessary shaft diameter.

Problem 9

A wind turbine with a cut-in velocity of 6 m/s and a cut-out velocity of 20 m/s is installed in a site where winds are Weibull-distributed with shape parameter k = 2.35 and scale parameter c = 9.8 m/s. How many hours in a 24-hour period will the wind turbine generate power?

(A) 23.3 h
(B) 20.1 h
(C) 17.5 h
(D) 14.3 h

Problem 10

Consider a single 60-m tall wind turbine that generates a noise level of 104 dB(A) at hub height. Assuming that sound radiates in a spherical pattern, and that the atmospheric sound absorption coefficient is 0.005 dB/m, what is the sound level received at a house located 900 m away from the base of the turbine?

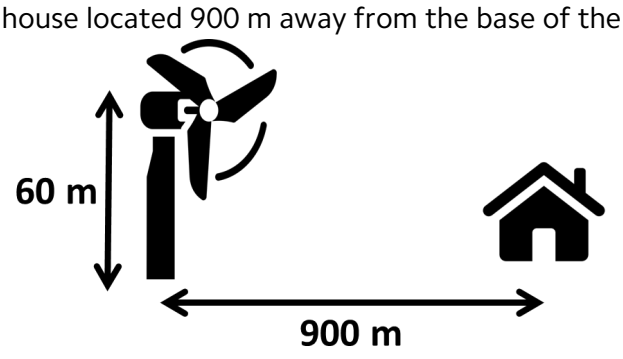

(A) 76.5 dB
(B) 54.4 dB
(C) 32.4 dB
(D) 21.6 dB

Problem 11

Regarding the theory of vertical-axis wind turbines (VAWTs), are the following statements true or false?

According to Korobenko *et al.* (2014), simulations of VAWTs are generally harder to implement than computational models of HAWTs. The reason is that even under steady wind and rotor speeds, the flow angle of attack of a VAWT is constantly changing, so the airflow across the vertical blades rapidly alternates between fully attached and separated. As a result, even under steady operating

conditions, this creates truly unsteady turbulent aerodynamics. High-fidelity modelling of the underlying aerodynamics requires a numerical formulation that properly accounts for this flow unsteadiness and is valid for all flow regimes present.

1.( ) Korobenko *et al.* (2014) conducted 3D finite-element simulations of a Darrieus-type three-blade, high-solidity VAWT. In order to overcome the issues of aerodynamic turbulence and unsteadiness mentioned above, Korobenko's group used a fine mesh with several million elements. While Korobenko's model is in good agreement with wind tunnel test data, their work, like so many reports in the wind energy literature, failed to address the inherently more complicated flow field produced when two or more VAWTs are placed side-by-side. ■

Recommended research: Korobenko *et al.* (2014).

2.( ) Howell *et al.* (2010) reported the results of CFD simulations and wind tunnel tests of a small-scale Darrieus-type VAWT. Two designs were considered, one with two blades (solidity = 0.67) and the other with three blades (solidity = 1.0). Howell's group observed that although the maximum torque per blade was very close for the two- and three-bladed designs, the power developed per blade was greater for the three-bladed model.

Recommended research: Howell *et al.* (2010).

Lee and Lim (2015) used CFD simulations based on Ansys FLUENT® to investigate optimal parameters for a Darrieus blade; variables studied included chord length, rotor diameter, pitch angle, blade thickness ratio, and helical angle. The simulations were complemented with wind tunnel tests in near-identical conditions.

3.( ) Importantly, Lee's group reported that increases in solidity yielded increasing torque and power coefficients irrespective of the range of tip-speed ratios considered. ■

Recommended research: Lee and Lim (2015).

4.( ) Adjustment of pitch angle in VAWTs has received significant attention from researchers because it is easy to apply in practice and does not introduce substantial manufacturing costs. However, results have been underwhelming. For one, Simão Ferreira and Scheurich (2014), investigating pitch angles of -3°, 0°, and 3°, found that although a shift in the instantaneous loads and moments was observed between the upwind and downwind sides of the turbine, the effect of pitch angle on the average loading coefficients was negligible. This finding was corroborated by Rezaeiha *et al.* (2017), who contested the existence of an optimal pitch angle and argued that zero pitch is preferable in most practical designs.

Recommended research: Simão Ferreira and Scheurich (2014); Rezaeiha *et al.* (2017).

Recent research on airfoil aerodynamics has produced at least two promising modifications that, albeit originally proposed for aviation purposes, may also find application in future VAWT designs. The first is a vertical flap known as *Gurney flap*, which was experimentally shown to improve lift coefficient with only a minor increase in drag. The second is the provision of dimples on the surface of an airfoil, so as to stimulate generation of vortices and ultimately enhance lift.

5.( ) Ismail and Vijayaraghavan (2015) brought these innovations to wind energy research by studying a NACA-0015 VAWT blade with both inward dimples and a Gurney flap at the lower surface, near the trailing edge. They showed that, when implemented in combination, these modifications can improve aerodynamic performance substantially. Importantly, Ismail's optimization routine sought to maximize effective torque instead of maximizing lift coefficient at a single angle of attack. ■

Recommended research: Ismail and Vijayaraghavan (2015).

Kjellin *et al.* (2011) described a Darrieus-type 12-kW VAWT built at Uppsala University, Sweden. Their H-rotor turbine design has 5-m high blades and 6 m diameter. It is passive-stall-controlled and has a shaft directly connecting turbine and rotor, a direct drive arrangement that enabled Kjellin's group to do away with a gearbox and its associated losses.

6.( ) Kjellin's group went on to report the peak power coefficient of their novel VAWT design; the value they published was greater than 0.25. ■

Recommended research: Kjellin *et al.* (2011).

Ahmadi-Baloutaki *et al.* (2016) conducted a series of wind tunnel experiments to study the aerodynamic interaction of VAWTs in group installations. Ahmadi-Baloutaki's group first experimented with two VAWTs placed side-by-side in a counterrotating fashion, and found a mild improvement in aerodynamic performance relatively to operation of a single turbine. Those workers went on to investigate the response of an additional VAWT positioned downstream of the counterrotating pair, and likewise found that this third turbine exhibited power generation superior to that of a lone turbine.

7.( ) Ahmadi-Baloutaki *et al.* (2016) also investigated a range of spacing parameters for their three-turbine array and reported that, over the range of studied conditions, the output power of a VAWT operating downstream of a counterrotating pair reached a local maximum when the streamwise distance from the pair to the third turbine was one rotor diameter, and the spacing between the two turbines of the pair was three rotor diameters. ■

Recommended research: Ahmadi-Baloutaki *et al.* (2016).

Few numerical studies have been undertaken to model the aerodynamic wake produced by VAWTs. One important contribution is the study of Lam and Peng (2016), who used two- and three-dimensional Ansys FLUENT® simulations to investigate the near- and far-wake characteristics of a straight-bladed VAWT. Stereoscopic particle image velocimetry (PIV) test data was used to validate the CFD modelling, and good agreement was obtained.

8.( ) In Lam's computational study, the two- and three-dimensional schemes predicted similar streamwise velocity deficits along the near- and far-wake. However, the 2D model fared somewhat poorly, overestimating streamwise velocity in the near wake and underestimating it in the far wake.

Recommended research: Lam and Peng (2016).

In an interesting application of biomimetics in wind energy research, Whittlesey *et al.* (2010) proposed a VAWT array configuration following the arrangement of shed vortices in the wake of schooling fish. Whittlesey's group was motivated by earlier findings that the reversed Kármán vortex street produced in the wake of a school of fish may lead to improved hydrodynamic performance.

9.( ) Whittlesey's group went on to compare their fish school-like VAWT array design with a similar configuration constituted of horizontal-axis turbines. Those authors found consistently superior power densities for VAWT farms when compared to analogous HAWT farms. ■

Recommended research: Whittlesey *et al.* (2010).

Solutions

■ Problem 1

1. False. The theoretical rated power of the turbine for one year is 2 MW × 8760 h = 17,520 MWh. If the turbine produced only 3600 MWh, the capacity factor *C* becomes

$$C = \frac{3600}{17{,}520} = 0.205 = \boxed{20.5\%}$$

2. True. This is a simple observational exercise. Entering a speed of 10 m/s into the graph, we read a power converted value of about 800 kW.

3. False. The turbulence intensity is obtained by dividing the component of wind speed at the direction of interest to its standard deviation; in the case at hand,

$$TI = \frac{\sigma_u}{\bar{u}} = \frac{2}{10} = \boxed{20\%}$$

4. True. The following table lists the residual fatigue strength at 10^8 cycles for four candidate blade materials. The fatigue performance of fiber composite materials is indeed superior.

Material	Residual strength at 10^8 cycles (MPa)
Glass-fiber reinf. comp.	95
Carbon-fiber reinf. comp.	449
High-strength steel	16
Wood-epoxy laminate	15

Reference: Anderson (2020).

5. False. In the DU family of airfoils, the two digits after DU refer to the year in which the airfoil was designed, while the three digits after W are 10 times the maximum thickness in percent of the chord. Accordingly, DU 93-W-210 was designed in 1993 and has a maximum thickness of 21%.

Reference: Timmer and van Rooij (2003).

6. False. Although three-bladed schemes with solidity ranging from 0.03 to 0.08 have been the mainstay of many current HAWT designs, the numerical models of Duquette and Visser (2003) actually indicated that maximum C_p values were observed for blade numbers of 6 to 12 and solidities ranging from 10 to 15%.

Reference: Duquette and Visser (2003).

7.False. The statement errs twice. Firstly, both wind shear models were reasonably accurate for flat terrain but fared poorly in sites with hills. Secondly, it was the log law, not the power law, that afforded more accurate results for sites with hills.

Reference: Ray *et al.* (2006).

8. True. Specifically, Dolan and Lehn (2006) showed that the wind-shear component of torque oscillations was most dependent on blade radius R, rotor hub elevation H, and wind shear exponent α; in turn, the tower shadow component was most dependent on R, tower radius a, and distance x from blade origin to tower midline. Importantly, there was no significant correlation between α and the total 3p pulsation, which was unsurprising given the fact that the wind-shear-induced component of pulsations amounted to only 5% of the tower-shadow-induced component.

Reference: Dolan and Lehn (2006).

9. False. Interestingly, Orlando *et al.* (2011) reported that velocity deficits were most pronounced when the anemometer was placed 2° – 5° from the centerline.

Reference: Orlando *et al.* (2011).

10. True. Gebraad *et al.* (2014) reported that their FAST solver yielded a reduced damage equivalent load (DEL) as a byproduct of yaw adjustment, even though this was not the objective of the simulation.

Reference: Gebraad *et al.* (2014).

11. False. Yang *et al.* (2019) actually used a simulated annealing algorithm (SAA), which, like PSO, is a metaheuristic optimization technique.

Reference: Yang *et al.* (2019).

12. False. Sørensen and Hansen (1998) noted that the rotor data and simulation results compared well for low speeds, but a distinct underprediction of mechanical power was registered for wind speeds above 10 m/s. They attributed this loss of accuracy to two factors. Firstly, they argued that mesh resolution undermined results because suction peaks become extremely narrow at high speeds, and failure to resolve the suction at high wind speeds may result in underprediction of mechanical power production. Secondly, they noted that at high speeds separation and turbulence become more pronounced, hence power production of the blade is no longer controlled by blade sections with attached flow; the inadequacy of the SST k-ω model in this region manifests as an erroneously predicted mechanical power.

Reference: Sørensen and Hansen (1998).

13. True. Indeed, Chou *et al.* (2013) noted that the blades can reliably resist forces induced by a wind speed as great as 80 m/s (288 km/h), which far exceeds the maximum instantaneous wind speed of 53.4 m/s (192 km/h) recorded during typhoon Jangmi. However, the actual wind turbine damage occurred mainly on the back edge of the blade near the wing section, where failure usually occurs as a result of damage to the junction between the surface layer and the cover layer; this indicates that material in this region has lower long-term durability. Chou's group noted that, regardless of whether the overall turbine blade can resist forces induced by high wind speeds, cracks and delamination between the junction faces of the cover layer caused by long-term wind effects are not properly considered in design guidelines. Accordingly, those authors recommend that suppliers provide data confirming that the cover layer material is sufficiently durable to prevent progressive damage of cover layers during normal operation and under typhoon-force winds.

Reference: Chou *et al.* (2013).

14. True. Li *et al.* (2014) conducted their experiments in the winter of 2012.

Reference: Li *et al.* (2014).

15. False. Mendez *et al.* (2015) indeed found that maximum lift coefficient decreased and minimum drag coefficient increased with rising *Re*; however, as the Reynolds number increased further into the turbulent region for the clean and rough conditions, the maximum lift coefficient actually increased and the drag coefficient decreased. This is in consonance with the review by Zidane *et al.* (2016), where it is stated that as the Reynolds number increases, the sensitivity of the airfoil to surface roughness decreases.

References: Mendez *et al.* (2015); Zidane *et al.* (2016).

16. True. By 'very small' we mean drops of diameter less than 0.3 mm, which Eisenberg *et al.* (2018) chose to ignore because of the greater uncertainty in their quantities in the air and the fact that these droplets occur as more of a 'mist' than a steady stream, thereby making their erosive activity harder to model.

Reference: Eisenberg *et al.* (2018).

17. True. As reviewed in Schuster *et al.* (2015), bats generally do not collide when turbines are non-operational. Collisions with other static anthropogenic structures, such as buildings or television towers, have been reported but are extremely rare, indicating that bat collision is strongly linked to blade movement. The high speeds associated with blade motion, especially close to the tip (~100 – 150 m/s), make it difficult for bats to avoid impact.

Reference: Schuster *et al.* (2015).

■ Problem 2

This is a straightforward application of the formula

$$V(z) = V(z_R)\frac{\ln(60/z_{OR})\ln(z/z_O)}{\ln(60/z_O)\ln(z_R/z_{OR})}$$

Substituting $V(z_R) = 8$ m/s, $z_{OR} = 0.05$ m (the roughness height at reference location), $z_O = 0.12$ m (the roughness height at the turbine site), $z_R = 10$ m (the height at the meteorological observatory) and $z = 35$ m, we find that

$$V(z) = 8 \times \frac{\ln(60/0.05)\times\ln(35/0.12)}{\ln(60/0.12)\times\ln(10/0.05)} = \boxed{9.78 \text{ m/s}}$$

➡ The correct answer is **B.**

■ Problem 3

The linear velocity at the tip is $v = V \times TSR = 8 \times 5 = 40$ m/s. The corresponding rotational speed is

$$v = \omega r \quad \rightarrow \quad \omega = \frac{v}{r}$$

$$\therefore \omega = \frac{40}{15} = 2.67 \text{ rad/s} = \boxed{25.5 \text{ rpm}}$$

➡ The correct answer is **D.**

■ Problem 4

The overall efficiency is

$$\eta = 0.95 \times 0.90 \times 0.28 = 0.239$$

The corresponding input power is

$$P_w = \frac{P_{\text{rated}}}{\eta} = \frac{2}{0.239} = 8.37 \text{ MW}$$

so that

$$P_w = \frac{1}{2}\rho A V^3 \quad \rightarrow \quad A = \frac{2P_w}{\rho V^3}$$

$$\therefore A = \frac{2\times(8.37\times10^6)}{1.225\times12^3} = \boxed{7910 \text{ m}^2}$$

➡ The correct answer is **B.**

■ Problem 5

We first compute the input power P_w,

$$P_w = \frac{1}{2}\rho A V^3 = \frac{1}{2}\times1.225\times\left(\frac{\pi\times50^2}{4}\right)\times14^3 = 3.30\times10^6 \text{ W}$$

The overall efficiency is determined as

$$\eta = \frac{1.8}{3.30} = 0.545$$

But

$$\eta = \eta_{gb}\eta_g C_P$$

so that, solving for power coefficient,

$$\eta = \eta_{gb}\eta_g C_P \quad \rightarrow \quad C_P = \frac{\eta}{\eta_{gb}\eta_g}$$

$$\therefore C_P = \frac{0.545}{0.98 \times 0.98} = \boxed{0.567}$$

Note that this is just below the Betz limit of ~0.593.

➡ The correct answer is **D.**

■ Problem 6

This is a straightforward application of the formula

$$R = \sqrt{\frac{P_{\text{rated}}}{\frac{1}{2}\rho V_{\text{rated}}^3 C_{P,\text{rated}}\pi}}$$

$$\therefore R = \sqrt{\frac{10^6}{0.5 \times 1.225 \times 15^3 \times 0.2 \times \pi}} = \boxed{27.7 \text{ m}}$$

■ Problem 7

Part 1: Knowing the actuator disk radius, the disk area becomes

$$A_d = \pi R_d^2 = \pi \times 5^2 = 78.5 \text{ m}^2$$

Noting that at the Betz limit, $C_p = 0.593$, the power extracted by the actuator disc becomes

$$P = C_P \times \frac{1}{2}\rho_a A_d V_\infty^3 = 0.593 \times \frac{1}{2} \times 1.225 \times 78.5 \times 8^3 = 14,600 \text{ W}$$

$$\therefore \boxed{P = 14.6 \text{ kW}}$$

Part 2: At the Betz limit, induction factor $a = 1/3$; the disc velocity is then

$$V_d = V_\infty (1-a) = 8 \times \left(1 - \frac{1}{3}\right) = \boxed{5.33 \text{ m/s}}$$

while at the wake,

$$V_w = V_\infty (1-2a) = 8 \times \left(1 - \frac{2}{3}\right) = \boxed{2.67 \text{ m/s}}$$

Part 3: Areas A_∞ and A_w can be calculated with the continuity equation, namely

$$(AV)_\infty = (AV)_d = (AV)_w$$

so that

$$A_\infty = \frac{A_d V_d}{V_\infty} = \frac{78.5 \times 5.33}{8} = \boxed{52.3 \text{ m}^2}$$

and

$$A_w = \frac{A_d V_d}{V_w} = \frac{78.5 \times 5.33}{2.67} = \boxed{157 \text{ m}^2}$$

■ Problem 8

Part 1: First of all, the power afforded by the incoming wind is

$$P_{\text{wind}} = \frac{P_t}{\eta} = \frac{1.2 \times 10^6}{0.40} = 3 \times 10^6 \text{ W}$$

Noting that the airspeed is $V = 32$ km/h = 8.89 m/s, we proceed to determine the swept area A:

$$P_{\text{wind}} = \frac{1}{2}\rho A V^3 \quad \rightarrow \quad A = \frac{2P_{\text{wind}}}{\rho V^3}$$

$$\therefore A = \frac{2\times\left(1.2\times10^6\right)}{1.225\times8.89^3} = 2790\ \text{m}^2$$

The rotor diameter follows as

$$A = \frac{\pi D^2}{4} \quad \rightarrow \quad D = \sqrt{\frac{4A}{\pi}}$$

$$\therefore D = \sqrt{\frac{4\times2790}{\pi}} = \boxed{59.6\ \text{m}}$$

The corresponding radius is R = 59.6/2 = 29.8 m. The rotational speed is

$$\omega = 20\times\frac{2\pi}{60} = 2.09\ \text{rad/s}$$

The tip-speed ratio follows as

$$TSR = \frac{\omega r}{V} = \frac{2.09\times29.8}{8.89} = \boxed{7.01}$$

Part 2: The torque is obtained by dividing the wind power P_{wind} by the rotational speed ω:

$$T = \frac{P}{\omega} = \frac{3\times10^6}{2.09} = \boxed{1.44\ \text{MN}\cdot\text{m}}$$

Then, appealing to the torsion formula,

$$\tau = \frac{TR_{\text{shaft}}}{J} = \frac{T\times R_{\text{shaft}}}{\frac{\pi R_{\text{shaft}}^4}{2}} = \frac{2T}{\pi R_{\text{shaft}}^3}$$

Solving for shaft radius brings to

$$\tau = \frac{2T}{\pi R_{\text{shaft}}^3} \quad \rightarrow \quad R_{\text{shaft}} = \left(\frac{2T}{\pi\tau}\right)^{\frac{1}{3}}$$

$$\therefore R_{\text{shaft}} = \left[\frac{2\times\left(1.44\times10^6\right)}{\pi\times\left(60\times10^6\right)}\right]^{\frac{1}{3}} = 0.248\ \text{m} = \boxed{24.8\ \text{cm}}$$

■ Problem 9

The number of hours that the wind turbine will operate is based on the probability that the wind speed falls between cut-in and cut-out values; in mathematical terms,

$$\Pr\left(V_6 < V < V_{20}\right) = \Pr\left(V_{20}\right) - \Pr\left(V_6\right)$$

$$\therefore \Pr\left(V_6 < V < V_{20}\right) = \exp\left[-\left(6/9.8\right)^{2.35}\right] - \exp\left[-\left(20/9.8\right)^{2.35}\right]$$

$$\therefore \Pr\left(V_6 < V < V_{20}\right) = 0.729 - 0.00477 = 0.724$$

Therefore, for a full day, the wind turbine will generate power in a number of hours equal to 0.729 × 24 = 17.5 h.

➡ The correct answer is **C.**

■ Problem 10

The sound propagates in a radial pattern along the radial vector, R. If the height of the turbine is H and the horizontal distance from the base of the tower to the house is D, we can write

$$R = \left(D^2 + H^2\right)^{1/2} = \left(900^2 + 60^2\right)^{1/2} = 902\ \text{m}$$

The sound level on the ground is given by

$$L_{W_p} = L_{W_*} - 10\log_{10}\left(2\pi R^2\right) - \alpha R$$

where L_{W_*} is the sound power level (dB) measured at the sound source, L_{W_P} is the propagated sound power level (dB) measured at the radial distance R from the sound source, and α is the frequency-dependent sound absorption coefficient; substituting the pertaining data gives

$$L_{W_p} = 104 - 10\times\log_{10}\left(2\pi\times902^2\right) - 0.005\times902 = \boxed{32.40\ \text{dB}}$$

➡ The correct answer is **C.**

■ Problem 11

1. False. Korobenko *et al.* (2014) actually included a case study of two counterrotating turbines placed side-by-side in close proximity. The wind and rotor speeds they used were the same as in the single-turbine case, but the turbines were positioned at an out-of-phase angular difference of 60 degrees.

Reference: Korobenko *et al.* (2014).

2. False. Howell *et al.* (2010) noted that although the maximum torque per blade was very close for the two- and three-bladed turbine models, the power per blade was higher for the two-blade turbine model because it developed the maximum torque at a higher rotational velocity. Howell's tests produced similar peaks in performance coefficient, but the three-bladed design did so at a much reduced tip speed ratio.

Reference: Howell *et al.* (2010).

3. False. Recall that solidity (σ) is the ratio of the length of blades to the rotor diameter, that is,

$$\sigma = \frac{\text{No. of blades} \times \text{Chord length}}{\text{Diameter of rotor}}$$

Lee and Lim (2015) went on to evaluate torque and power coefficients for three different chord lengths (100, 150, 200 mm) corresponding to three values of solidity (0.4, 0.6, 0.8). They found that when the tip-speed ratio is 2 or less, the rotor with the chord length of 200 mm (i.e., the one with the highest solidity) had the highest torque and power coefficients. On the other hand, when the TSR is 2.4 or higher, the rotor with the chord length of 100 mm (i.e., the one with the lowest solidity) exhibited the highest torque and power coefficients.

Reference: Lee and Lim (2015).

4. False. While it is true that Simão Ferreira and Scheurich (2014) found negligible differences in load coefficients for the pitch angles they tested, Rezaeiha *et al.* (2017) argued that there may exist an optimum fixed blade angle that enhances VAWT performance, although its exact value of course varies from one design to another. In the VAWT design that Rezaeiha's group worked with, a fixed pitch angle of -2° improved performance by 6.6% relatively to operation at zero pitch.

References: Simão Ferreira and Scheurich (2014); Rezaeiha *et al.* (2017).

5. True. As the angle of attack of the blades in a VAWT changes continuously even when the wind speed and rotation remain constant, Ismail and Vijayaraghavan (2015) attempted to maximize effective torque instead of maximizing the lift coefficient at a single angle of attack.

Reference: Ismail and Vijayaraghavan (2015).

6. True. Kjellin *et al.* (2011) reported that the power coefficient of their VAWT design peaked at 0.29 for a tip speed ratio of 3.3.

Reference: Kjellin *et al.* (2011).

7. False. Swap 'one diameter' with 'three diameters' and you'll get a correct statement; Ahmadi-Baloutaki *et al.* (2016) actually reported that

over the range of studied conditions, the output power of a vertical axis wind turbine operating downstream of a counterrotating pair reached a local maximum when the streamwise distance from pair was three rotor diameters, and the spacing between two turbines of the pair was one rotor diameter.

Reference: Ahmadi-Baloutaki *et al.* (2016, verbatim from section 4).

8. True. Lam and Peng (2016) hypothesized that the infinite blade depth and tower height in the two-dimensional model led to a higher effective approaching velocity and hence explained the overestimation observed in the near wake. Moreover, the two-dimensional model cannot account for vortical motions at the blade tips, and results from the 3D simulation suggest that these types of motion are critical in the VAWT's wake development.

Reference: Lam and Peng (2016).

9. True. Indeed, Whittlesey *et al.* (2010) indicated that significantly higher power densities are obtained with VAWT farms compared to operational HAWT farms in a similar fish-school-like arrangement.

Reference: Whittlesey *et al.* (2010).

Answer Summary

Problem 1	T/F
Problem 2	B
Problem 3	D
Problem 4	B
Problem 5	D
Problem 6	C
Problem 7	Open-ended pb.
Problem 8	Open-ended pb.
Problem 9	C
Problem 10	C
Problem 11	T/F

References

- Ahmadi-Baloutaki, M., Carriveau, R. and Ting, D.S.-K. (2016). A wind tunnel study on the aerodynamic interaction of vertical axis wind turbines in array configurations. *Renew Energ*, 96(A), 904 – 913. DOI: 10.1016/j.renene.2016.05.060
- ANDERSON, C.G. (2020). *Wind Turbines: Theory and Practice*. Cambridge: Cambridge University Press.
- Chou, J.-S., Chiu, C.-K.Huang, I-K. and Chi, K.-N. (2013). Failure analysis of wind turbine blade under critical wind loads. *Eng Fail Anal*, 27, 99 – 118. DOI: 10.1016/j.engfailanal.2012.08.002
- Dolan, D.S.L. and Lehn, P.W. (2006). Simulation model of wind turbine 3p torque oscillations due to wind shear and tower shadow. *IEEE Trans Energy Convers*, 21(3), 717 – 724. DOI: 10.1109/TEC.2006.874211
- Duquette, M.M. and Visser, K.D. (2003). Numerical implications of solidity and blade number on rotor performance of horizontal-axis wind turbines. *J Sol Energy Eng*, 125(4), 425 – 432. DOI: 10.1115/1.1629751
- Eisenberg, D., Lautsen, S. and Stege, J. (2018). Wind turbine blade coating leading edge rain erosion model: Development and validation. *Wind Energ*, 21(18), 942 – 951. DOI: 10.1002/we.2200
- Gebraad, P.M.O., Teeuwisse, F.W., van Wingerden, J.W. *et al.* (2014) Wind plant power optimization through yaw control using a parametric model for wake effects – a CFD simulation study. *Wind Energ*, 19(1), 95 – 114. DOI: 10.1002/we.1822
- Howell, R., Qin, N., Edwards, J. and Durrani, N. (2010). Wind tunnel and numerical study of a small vertical axis wind turbine. *Renew Energ*, 35(2), 412 – 422. DOI: 10.1016/j.renene.2009.07.025
- Ismail, M.F. and Vijayaraghavan, K. (2015). The effects of aerofoil profile modification on a vertical axis wind turbine performance. *Energy,* 80, 20 – 31. DOI: 10.1016/j.energy.2014.11.034
- Kjellin, J., Bülow, F., Eriksson, S. *et al.* (2011). Power coefficient measurement on a 12-kW straight bladed vertical axis wind turbine. *Renew Energ,* 36(11), 3050 – 3053. DOI: 10.1016/j.renene.2011.03.031Get
- Korobenko, A., Hsu, M.-C. and Bazilevs, A.Y. (2014). Aerodynamic simulation of vertical-axis wind turbines. *J Appl Mech*, 81(2), 021011. DOI: 10.1115/1.4024415
- Lam, H.F. and Peng, H.Y. (2016). Study of wake characteristics of a vertical axis wind turbine by two- and three-dimensional computational fluid dynamics simulations. *Renew Energ*, 90, 386 – 398. DOI: 10.1016/j.renene.2016.01.011
- Lee, Y.-T. and Lim, H.-C. (2015). Numerical study of the aerodynamic performance of a 500 W Darrieus-type vertical-axis wind turbine. *Renew Energ*, 83, 407 – 415. DOI: 10.1016/j.renene.2015.04.043
- Li, Y., Tagawa, K., Feng, F. *et al.* (2014). A wind tunnel experimental study of icing on wind turbine blade airfoil. *Energy Convers Manag*, 85, 591 – 595. DOI: 10.1016/j.enconman.2014.05.026
- Mendez, B., Muñoz, A. and Munduate, X. (2015). Study of distributed roughness effect over wind turbine airfoils performance using CFD. *33rd Wind Energy Symposium*, Kissimmee, 5 – 9 January 2015. DOI: 10.2514/6.2015-0994
- Orlando, S., Bale, A. and Johnson, D.A. (2011). Experimental study of the effect of tower shadow on anemometer readings. *J Wind Eng Ind Aerodyn*, 99(1), 1 – 6. DOI: 10.1016/j.jweia.2010.10.002

- Ray, M.L., Rogers, A.L. and McGowan, J.G. (2006). Analysis of wind shear models and trends in different terrains. University of Massachusetts, Amherst. Available at: https://www.researchgate.net/publication/251965566_Analysis_of_wind_shear_models_and_trends_in_different_terrain
- Rezaeiha, A., Kalkman, I. and Blocken, B. (2017). Effect of pitch angle on power performance and aerodynamics of a vertical axis wind turbine. *Appl Energy*, 197, 132 – 150. DOI: 10.1016/j.apenergy.2017.03.128
- Schuster, E., Bulling, L. and Köppel, J. (2015). Consolidating the state of knowledge: A synoptical review of wind energy's wildlife effects. *Environ Manag*, 56, 300 – 331. DOI: 10.1007/s00267-015-0501-5
- Simão Ferreira, C. and Scheurich, F. (2014). Demonstrating that power and instantaneous loads are decoupled in a vertical-axis wind turbine. *Wind Energ*, 17(3), 385 – 396. DOI: 10.1002/we.1581
- Sørensen, N. and Hansen, M. (1998). Rotor performance predictions using a Navier-Stokes method. *1998 ASME Wind Energy Symposium*, Reno, 12 – 15 January 1998. DOI: 10.2514/6.1998-25
- Timmer, W.A. and van Rooij, R.P.J.O.M. (2003). Summary of the Delft University wind turbine dedicated airfoils. *J Sol Energy Eng*, 125(4), 488 – 496. DOI: 10.1115/1.1626129
- Whittlesey, R.W., Liska, S. and Dabiri, J.O. (2010). Fish schooling as a basis for vertical axis wind turbine farm design. *Bioinsp Biomim*, 5(3), 035005. DOI: 10.1088/1748-3182/5/3/035005
- Yang, K., Kwak, G., Cho, K. and Huh, J. (2019). Wind farm layout optimization for wake effect uniformity. *Energy*, 183, 983 – 995. DOI: 10.1016/j.energy.2019.07.019
- Zidane, I.F., Saqr, K.M., Swadener, G. *et al.* (2016). On the role of surface roughness in the aerodynamic performance and energy conversion of horizontal wind turbine blades: a review. *Int J Energy Res*, 40(15), 2054 – 2077. DOI: 10.1002/er.3580